the plant journal

SEB SOCIETY FOR EXPERIMENTAL BIOLOGY

The Plant Journal (2022) **111,** 966–978 doi: 10.1111/tpj.15864

OsIRO3 negatively regulates Fe homeostasis by repressing the expression of *OsIRO2*

Chenyang Li[1,2] , Yang Li[1,2] , Peng Xu[1,2] and Gang Liang[1,2,*]

[1]*CAS Key Laboratory of Tropical Plant Resources and Sustainable Use, The Xishuangbanna Tropical Botanical Garden, Innovative Academy of Seed Design, Chinese Academy of Sciences, Kunming, Yunnan 650223, China, and*

[2]*The College of Life Sciences, University of Chinese Academy of Sciences, Beijing 100049, China*

Received 12 February 2022; revised 27 April 2022; accepted 7 June 2022.; published online 11 June 2022.

*For correspondence (e-mail lianggang@xtbg.ac.cn).

SUMMARY

Iron (Fe) is crucial for crop productivity and quality. However, Fe deficiency is prevalent worldwide, particularly in alkaline soil. Plants have evolved sophisticated mechanisms to withstand Fe-deficient conditions. *Oryza sativa* IRON-RELATED BHLH TRANSCRIPTION FACTOR 3 (OsIRO3/OsbHLH63) has been identified as a negative regulator of Fe deficiency response signaling; however, the underlying mechanism remains unclear. In the present study, we constructed two *iro3* mutants, which developed leaves with necrotic lesions under Fe-deficient conditions. Loss-of-function of *OsIRO3* caused upregulation of Fe deficiency-associated genes in the root. Fe concentration measurements showed that the *iro3* mutants had increased shoot Fe concentration only under Fe-deficient conditions. Further analysis revealed that OsIRO3 directly regulated the expression of *IRON-RELATED BHLH TRANSCRIPTION FACTOR 2* (*OsIRO2*), which encodes a positive regulator of the Fe uptake system. Further investigation demonstrated that OsIRO3 interacted with POSITIVE REGULATOR OF IRON HOMEOSTASIS 1(OsPRI1) and OsPRI2, and. OsIRO3 repressed their transcription activation towards *OsIRO2*. OsIRO3 contains an EAR motif, which recruits the TOPLESS/TOPLESS-RELATED (OsTPL/OsTPRs) corepressors. Mutation of the EAR motif attenuated the repression ability of OsIRO3. This work sheds light on the molecular mechanism by which OsIRO3 modulates Fe homeostasis in rice.

Keywords: iron, OsIRO3, OsIRO2, OsFIT, OsPRI1, OsPRI2.

INTRODUCTION

Iron (Fe) is one of the indispensable micronutrients for plant growth and development, which is involved in many physiological and biochemical reactions such as photosynthesis, mitochondrial respiration, hormone biosynthesis and nitrogen fixation (Balk & Schaedler, 2014; Hänsch & Mendel, 2009). Although Fe is abundant on earth, its availability is limited due to the low solubility at alkaline pH (Mori, 1999). Calcareous soil accounts for about one-third of the world's cultivated soil, making Fe deficiency a very common phenomenon (Guerinot & Yi, 1994). Fe deficiency often leads to interveinal chlorosis of leaves, as well as greatly affecting the yield and nutritional quality of crops (Briat et al., 2015). Reactive oxygen radicals produced by excess Fe are toxic to plant cells (Valko et al., 2005). Therefore, the Fe concentration in plant cells needs to be regulated strictly.

To cope with Fe deficiency, plants have developed complicated molecular mechanisms for Fe uptake, translocation and storage to meet the Fe demand. Plants have evolved different strategies to absorb Fe (Römheld & Marschner, 1986). Gramineous plants employ a chelation strategy to acquire Fe. They excrete mugineic acid (MAs) family phytosiderophores to chelate Fe^{3+} to form the MA-Fe^{3+} complex, which is translocated into roots by YS/YSL transporters. In rice, the synthesis of MAs is mediated by a series of enzymes, including *S*-adenosylmethionine synthetase, nicotianamine synthase (NAS), nicotianamine aminotransferase (NAAT), and deoxymugineic acid synthase (DMAS) (Bashir et al., 2017; Mori, 1999; Shojima et al., 1990). The efflux of MAs from roots counts on TRANSPORTER OF MAs 1 (OsTOM1) (Nozoye et al., 2011) and the influx of Fe^{3+}-MA to roots involves YELLOW STRIP LIKE 15 (OsYSL15) (Inoue et al., 2009; Lee et al., 2009). In addition to the chelation strategy, rice plants also directly acquire Fe^{2+} by the Fe^{2+} transporter OsIRT1 (Ishimaru et al., 2006).

The Fe deficiency response is under the control of a series of transcription factors, which constitute a complex

regulatory network. IRON-RELATED BHLH TRANSCRIPTION FACTOR 2 (OsIRO2) is a key positive transcription factor of Fe homeostasis, which positively modulates the expression of chelation strategy associated genes, including *OsNAS1*, *OsNAS2*, *OsNAAT1*, *OsDMAS1*, *OsTOM1*, and *OsYSL15* (Liang et al., 2020; Ogo et al., 2007; Wang, Li, et al., 2020). *Oryza sativa* FER-LIKE FE DEFICIENCY-INDUCED TRANSCRIPTION FACTOR (OsFIT)/OsbHLH156 was identified as an interacting partner of OsIRO2. OsIRO2 protein mainly localizes to the cytoplasm, and OsFIT can facilitate the nuclear accumulation of OsIRO2 under Fe limited conditions (Liang et al., 2020; Wang, Li, et al., 2020). OsFIT and OsIRO2 interdependently regulate the expression of chelation strategy associated genes (Liang et al., 2020). *OsIRO2* is inducible by Fe deficiency both in the root and shoot (Ogo et al., 2007), and its upregulation is dependent on *Oryza sativa* POSITIVE REGULATOR OF IRON HOMEOSTASIS (OsPRI) proteins, OsPRI1 (OsbHLH060), OsPRI2 (OsbHLH058), and OsPRI3 (OsbHLH059) (Kobayashi et al., 2019; Zhang et al., 2017, 2020). *Oryza sativa* HEMERYTHRIN MOTIF-CONTAINING REALLY INTERESTING NEW GENE AND ZINC-FINGER PROTEIN1 (OsHRZ1) and OsHRZ2 negatively regulate the expression of Fe deficiency inducible genes (Kobayashi et al., 2013). OsHRZ1 possesses a RING domain responsible for its E3 ligase activity. Recently, it is established that OsHRZ1 interacts with OsPRI1/2/3 and promotes the degradation of the latter (Zhang et al., 2017, 2020).

OsIRO3 was identified as a nuclear-localized negative regulator of Fe homeostasis (Zheng et al., 2010). Similar to OsIRO2, OsIRO3 is also inducible under Fe-deficient conditions and directly regulated by OsPRI1/2/3 (Kobayashi et al., 2019; Zhang et al., 2017, 2020). Overexpression of *OsIRO3* causes leaf chlorosis, reduced shoot Fe concentration, and downregulation of Fe deficiency inducible genes (Zheng et al., 2010). Recently, two different groups generated and analyzed *iro3* loss-of-function mutants (Wang, Itai, et al., 2020; Wang, Ye, et al., 2020). Wang, Itai, et al. (2020) showed that the expression of Fe deficiency inducible genes increased in the root of *iro3* mutants, but Wang, Ye, et al. (2020) showed that OsIRO3 regulates only *OsNAS3*, but not other Fe deficiency inducible genes. Moreover, the underlying molecular mechanism by which OsIRO3 regulates Fe homeostasis remains unclear. In the present study, we showed that the loss-of-function of *OsIRO3* caused the upregulation of many Fe deficiency inducible genes in the root. Further investigation found that OsIRO3 directly binds to and inhibits the promoter of *OsIRO2*. On the other hand, OsIRO3 physically interacts with OsPRI1/2 and represses the transactivation ability of the latter to *OsIRO2*. In addition, OsIRO3 contains an EAR motif recruiting the OsTPL/OsTPRs corepressors, which partially accounts for its repression function.

RESULTS

Loss-of-function of *OsIRO3* impairs the Fe deficiency response

To clarify further the functions of OsIRO3 in the Fe deficiency response, we generated two *iro3* loss-of-function mutants with the CRISPR-Cas9 gene editing system. Two independent lines, *iro3-del1* with a deletion of nucleotide T in exon 4 and *iro3-del61* with a deletion of 61 bp in exon 3 were selected for further analysis (Figure 1a). Under Fe sufficient conditions, wild-type and *iro3* mutant plants showed no discernable differences (Figure 1b). Under Fe-deficient conditions, the wild-type plants displayed the typical Fe deficiency symptom, chlorotic leaves. In contrast, 3 days after transfer to the Fe deficiency medium, the mutants developed brown necrotic lesions in leaves, and the necrotic lesions gradually increased with the duration of Fe deficiency treatment. Meanwhile, compared with the wild-type plants, the mutant plants developed dwarf shoots (Figure 1b). To explore whether loss-of-function of *OsIRO3* affects Fe homeostasis, we measured the Fe concentration in the root and shoot. Although the Fe concentration in the root and shoot of *iro3* mutants was not significantly different from that in the wild type under Fe-sufficient conditions, the shoot Fe concentration in the *iro3* mutants was higher than that in the wild-type plants under Fe-deficient conditions (Figure 1c), indicating that Fe translocation from root to shoot was enhanced in the *iro3* mutants. Collectively, these data suggest that loss-of-function of *OsIRO3* leads to the disruption of Fe homeostasis.

Loss-of-function of *OsIRO3* results in the activation of OsIRO2 regulon

Given that the loss of *OsIRO3* function disrupted the Fe homeostasis of rice, we wondered whether the expression of Fe deficiency inducible genes was changed in the *iro3* mutants. Therefore, we detected the gene expression of several representative Fe deficiency inducible genes. OsIRO2 and OsFIT are the master regulators of the Fe deficiency response, which positively regulate not only the Strategy II associated genes (Liang et al., 2020; Ogo et al., 2007; Wang, Li, et al., 2020), such as *OsNAS1*, *OsNAS2*, *OsNAAT1*, and *OsDMAS1*, which encode the enzymes responsible for DMA synthesis (Bashir et al., 2017; Cheng et al., 2007; Inoue et al., 2003), *OsTOM1*, product of which accounts for the excretion of DMA (Nozoye et al., 2011), and *OsYSL15*, which encodes an Fe(III)-DMA transporter (Inoue et al., 2009; Lee et al., 2009), but also the Strategy I associated gene *OsIRT1* (Ishimaru et al., 2006). When rice plants are Fe deficient they initiate the expression of these genes. We found that the expression of *OsIRO2* and *OsFIT* and their downstream genes was considerably enhanced in the *iro3* root under

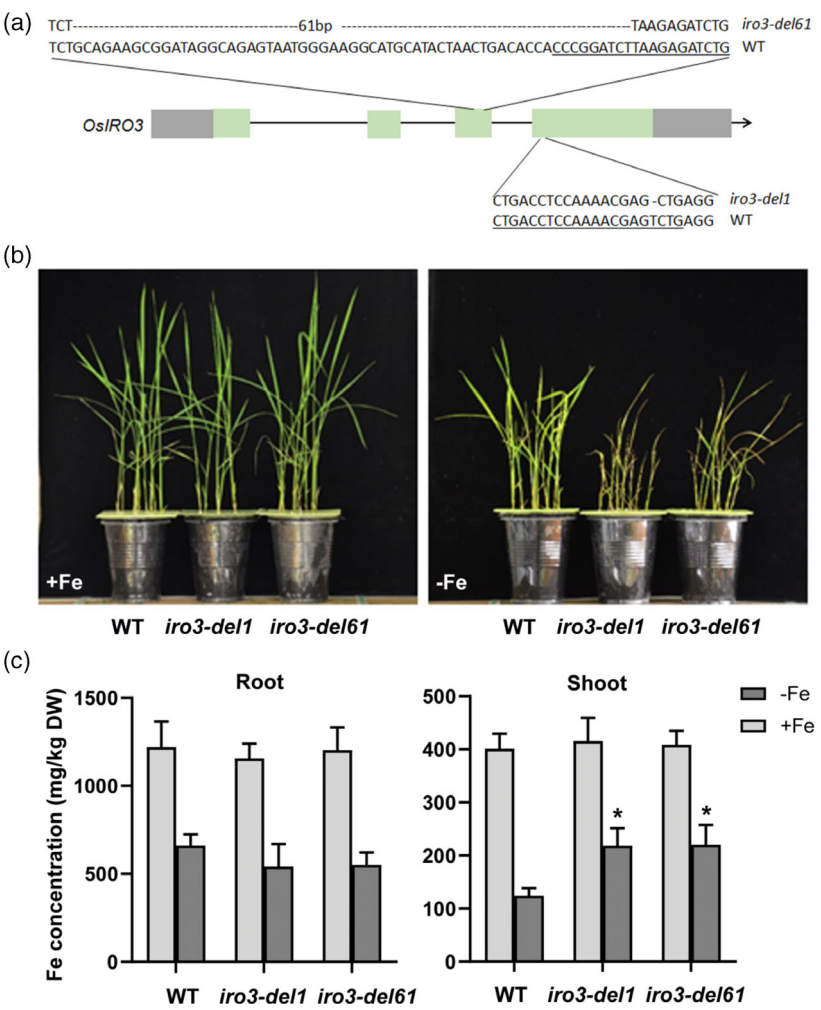

Figure 1. Identification of *iro3* mutants.
(a) Mutations generated in the *iro3* mutants by CRISPR/Cas9. Underlined letters indicate the target site. The *iro3-del1* mutant contains a deletion of nucleotide T in exon 4 and the *iro3-del61* mutant contains a deletion of 61 bp in exon 3. The genotypes of *iro3-del1* and *iro3-del61* are indicated.
(b) Phenotypes of *iro3* mutants. Seeds were grown in +Fe (0.1 mM Fe^{3+}) solution for 2 weeks, and then shifted to +Fe or −Fe (Fe free) solution for 1 week.
(c) Fe concentration in the *iro3* mutants. Two-week-old seedlings grown in +Fe were transferred to +Fe or −Fe solution for 1 week. Shoots and roots were separately sampled and used for metal measurement. Error bars represent the SD ($n = 3$). Value that is significantly different from the corresponding wild-type (WT) value was indicated by $^*P < 0.05$, as determined by Student's *t* test. DW, dry weight.

both Fe-sufficient and Fe-deficient conditions, which is consistent with the negative function of OsIRO3 (Figure 2). These results suggest that the expression of Fe deficiency inducible genes is disrupted in the *iro3* mutants.

OsIRO3 directly represses the expression of *OsIRO2*

Given that *OsIRO2* and *OsFIT* and their downstream genes are downregulated in the *OsIRO3* overexpression plants (Zheng et al., 2010), and upregulated in the *iro3* plants (Figure 2), we speculated that OsIRO3 might directly regulate the expression of *OsIRO2* and *OsFIT*. The bHLH family transcription factors can bind to the E-box motifs within their target DNA (Fisher & Goding, 1992). Several E-box motifs (CANNTG) exist in the promoters of *OsIRO2* and *OsFIT* (Figure S1; Zhang et al., 2017, 2020). Electrophoresis mobility shift assays (EMSAs) were performed to test whether OsIRO3 directly binds to the promoters of *OsIRO2* and *OsFIT*. 6xHis (histidine) tagged OsIRO3 (His-OsIRO3) was expressed and purified from *Escherichia coli*. When His-OsIRO3 was incubated with the biotin-labeled *OsIRO2* promoter probe, a prominent DNA-protein complex was detected. The binding capacity decreased as the wild-type unlabeled probe increased; however, the addition of the mutated wild-type unlabeled probe without an E-box did not affect the abundance of the DNA-protein complex (Figure 3a). The same EMSAs were conducted using the *OsFIT* promoter probe, indicating that OsIRO3 could not bind to the *OsFIT* promoter (Figure S1). These results suggest that OsIRO3 directly associates with the promoter of *OsIRO2*, but not of *OsFIT*.

To investigate whether OsIRO3 directly binds to and represses the promoter of *OsIRO2*, we prepared a reporter plasmid, Pro_{IRO2}:*nGFP*, in which a nuclear localization signal fused *GFP* (*nGFP*) was driven by the 2204 bp upstream region of *OsIRO2* (Figure 3b). For the effector plasmids, MYC-tagged OsPRI1 and OsIRO3 were respectively cloned downstream of the 35S promoter. Transient expression assays were performed in tobacco leaves (Figure 3c). As the promoter activity directly relates to the transcription of GFP, we determine the expression of GFP. As a positive control, OsPRI1 significantly activated the expression of *GFP*. In contrast, OsIRO3 repressed the expression of *GFP*.

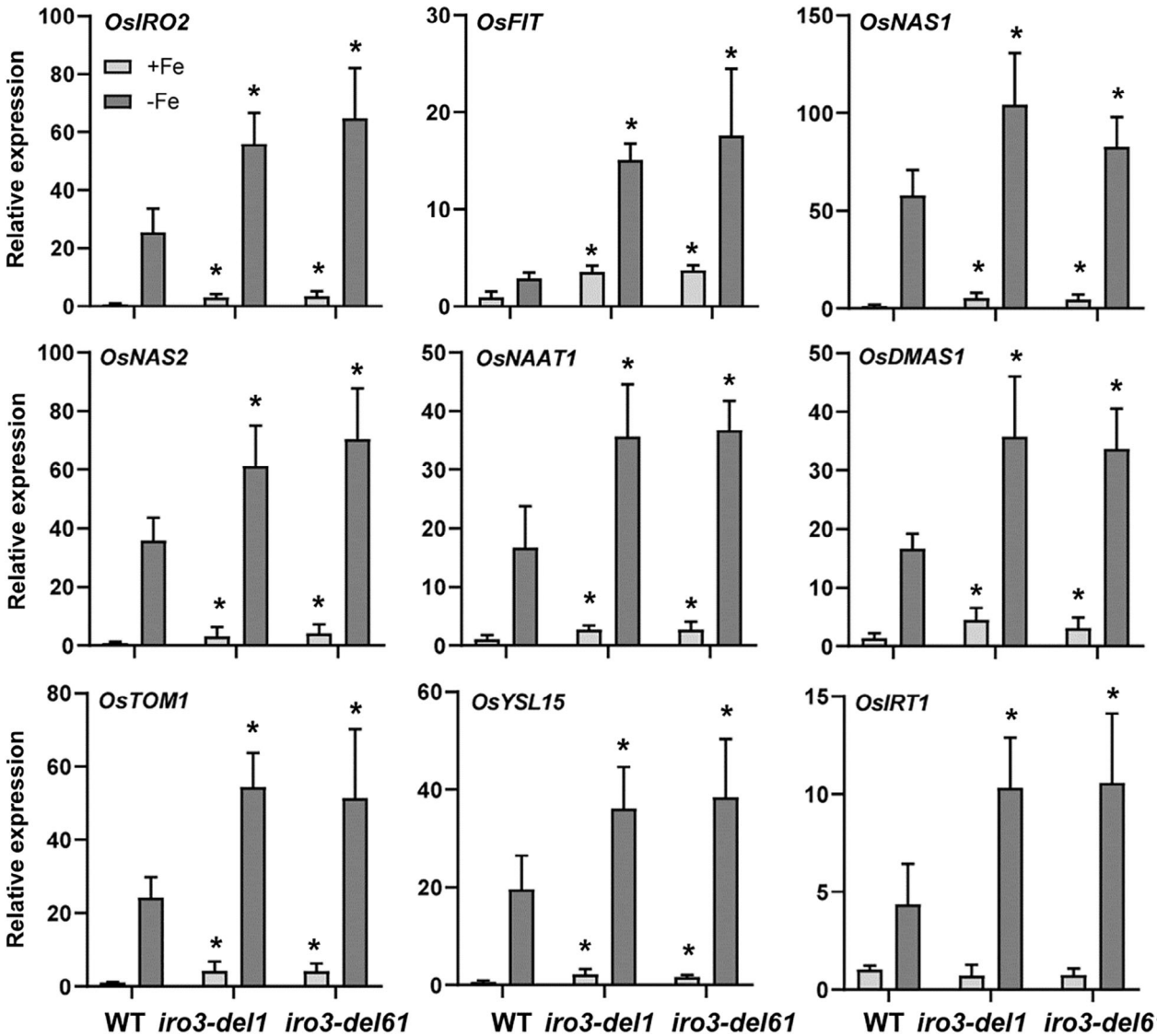

Figure 2. Expression of Fe deficiency inducible genes in the *iro3* mutants.
Two-week-old seedlings grown in +Fe solution were transferred to +Fe or −Fe solution for 7 days. Roots were sampled and used for RNA extraction. Numbers above the bars indicate the corresponding mean values. Error bars represent the SD ($n = 3$). The value that is significantly different from the corresponding wild-type (WT) value was indicated by $*P < 0.05$, as determined by Student's *t* test.

These results indicate that OsIRO3 directly binds to and represses the *OsIRO2* promoter.

OsIRO3 interacts with OsPRI1 and OsPRI2

Generally, bHLH transcription factors regulate downstream target genes by forming homodimers or heterodimers (Toledo-Ortiz et al., 2003). Considering that the Fe deficiency inducible genes regulated by OsIRO3 are also regulated by OsPRIs (OsPRI1, OsPRI2, and OsPRI3) (Zhang et al., 2017; Zhang et al., 2020), we speculated that OsIRO3 interacts with OsPRIs to form heterodimers to modulate the Fe deficiency response.

Yeast two-hybrid assays were used to test the potential protein interactions. As the strong self-activation of the full-length OsIRO3, the N-terminal part of OsIRO3 (OsIRO3n) containing the bHLH domain was fused with the GAL4 DNA-binding domain (BD) as the bait. Four OsPRIs were respectively fused to the GAL4 activating domain as prey. Yeast two-hybrid assays showed that OsPRI1 and OsPRI2, but not OsPRI3 and OsPRI4, interact with OsIRO3 (Figure 4a). To verify further the interactions between OsIRO3 and OsPRI1/2, pull-down assays were carried out. OsPRI1 and OsPRI2 were fused with the glutathione *S*-transferase (GST) tag respectively, and OsIRO3 was fused with the 6xHis tag. Proteins were expressed and purified from *E. coli*. GST, GST-OsPRI1, and GST-OsPRI2 were respectively co-incubated with His-tagged OsIRO3 and then eluted. The immunoblot results showed that GST-OsPRI1

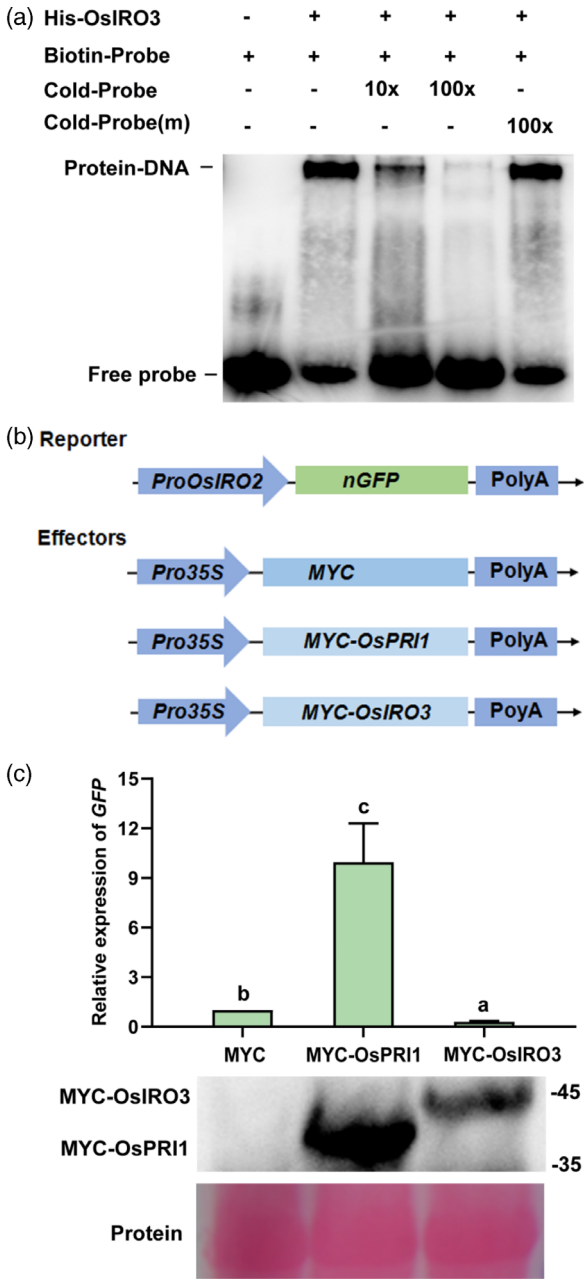

Figure 3. OsIRO3 binds to the promoter of *OsIRO2*.
(a) EMSA assays. Biotin-labeled DNA probe was incubated with the recombinant His-OsIRO3 protein. An excess of unlabeled probe (Cold-Probe) or unlabeled mutated probe (Cold-Probe-m) was added to compete with labeled probe (Biotin-Probe). Biotin-probe incubated with His protein served as the negative control.
(b) Schematic representation of the constructs used for transient expression assays. In the reporter, the *OsIRO2* promoter was used to drive a nuclear localization sequence fused GFP (nGFP). In the effectors, MYC, MYC-OsPRI1, and MYC-OsIRO3 are under the control of the cauliflower mosaic virus (CaMV) 35S promoter.
(c) *GFP* transcript abundance. Protein levels of effectors were detected by immunoblot. Ponceau staining shows equal loading. *GFP* transcript abundance was normalized to *NPTII* transcript. The value with the empty vector (MYC) as an effector was set to 1. Different letters above each bar indicate statistically significant differences as determined by one-way ANOVA followed by Tukey's multiple comparison test ($P < 0.05$).

and GST-OsPRI2 pulled down His-OsIRO3, but GST did not (Figure 4b). To verify further whether their interactions also occur in plant cells, tripartite split-GFP assays were performed in *Nicotiana benthamiana* leaves. The GFP10 fragment was fused with the N-end of OsIRO3 (GFP10-OsIRO3) and the GFP11 fragment with the C-end of OsPRI1/2 (OsPRI1/2-GFP11). When OsPRI1-GFP11 (or OsPRI2-GFP11) was co-expressed with GFP10-OsIRO3 and GFP1-9, the strong fluorescence signal was detected in the nucleus, whereas the fluorescence signal was hardly detected in the cells co-expressing GFP11, GFP10-OsIRO3, and GFP1-9 (Figure 4c). All these results indicate that OsIRO3 interacts with OsPRI1 and OsPRI2.

OsIRO3 inhibits the transactivation of OsPRI1 towards *OsIRO2*

It has been established that OsPRI1/2/3 positively regulate the expression of *OsIRO2* through directly binding to and activating its promoter (Zhang et al., 2017, 2020). Considering that OsIRO3 interacts with OsPRI1/2, we wanted to know whether OsIRO3 interferes with the transactivation ability of OsPRI1/2 towards *OsIRO2*. We carried out transient expression assays using the above-mentioned reporter-effector system (Figure 3b). Compared with the control effector (MYC), the co-expression of OsIRO3 with OsPRI1 significantly weakened the GFP signal (Figure 5a). These data suggest that OsIRO3 inhibits the transactivation of OsPRI1 towards *OsIRO2*.

To clarify further whether OsIRO3 directly represses the transactivation function of OsPRI1 by protein interaction, we employed the GAL4-based reporter-effector system (Li et al., 2022). For the reporter, the *nGFP* was driven by a synthetic promoter, which consists of five repeats of GAL4 binding motif and the minimal CaMV 35S promoter (Figure 5b). For the effector, the GAL4 BD fused with an NLS-mCherry and OsPRI1 was driven by the 35S promoter (Figure 5b). Compared with the control (nmCherry), OsPRI1 activated the expression of *GFP* (Figure 5c). When OsIRO3 was co-expressed with OsPRI1, the expression of *GFP* was significantly suppressed. These data suggest that OsIRO3 inhibits the transactivation of OsPRI1 through the direct protein interaction with OsPRI1.

OsIRO3 interacts with the co-repressors OsTPL/OsTPRs

Many negative transcription factors exert the repression function by their EAR recruiting transcriptional co-repressors TOPLESS/TOPLESS-RELATED (TPL/TPRs). Two types of EAR motifs, LxLxL and DLNxxP, have been characterized (Causier et al., 2012; Kagale et al., 2010). We found that both OsIRO2 and OsIRO3 contain a typical LxLxL EAR motif (Figure 6a).

Subsequently, we wondered whether both OsIRO2 and OsIRO3 could interact with OsTPL/OsTPRs. We employed the yeast two-hybrid assays to test their protein

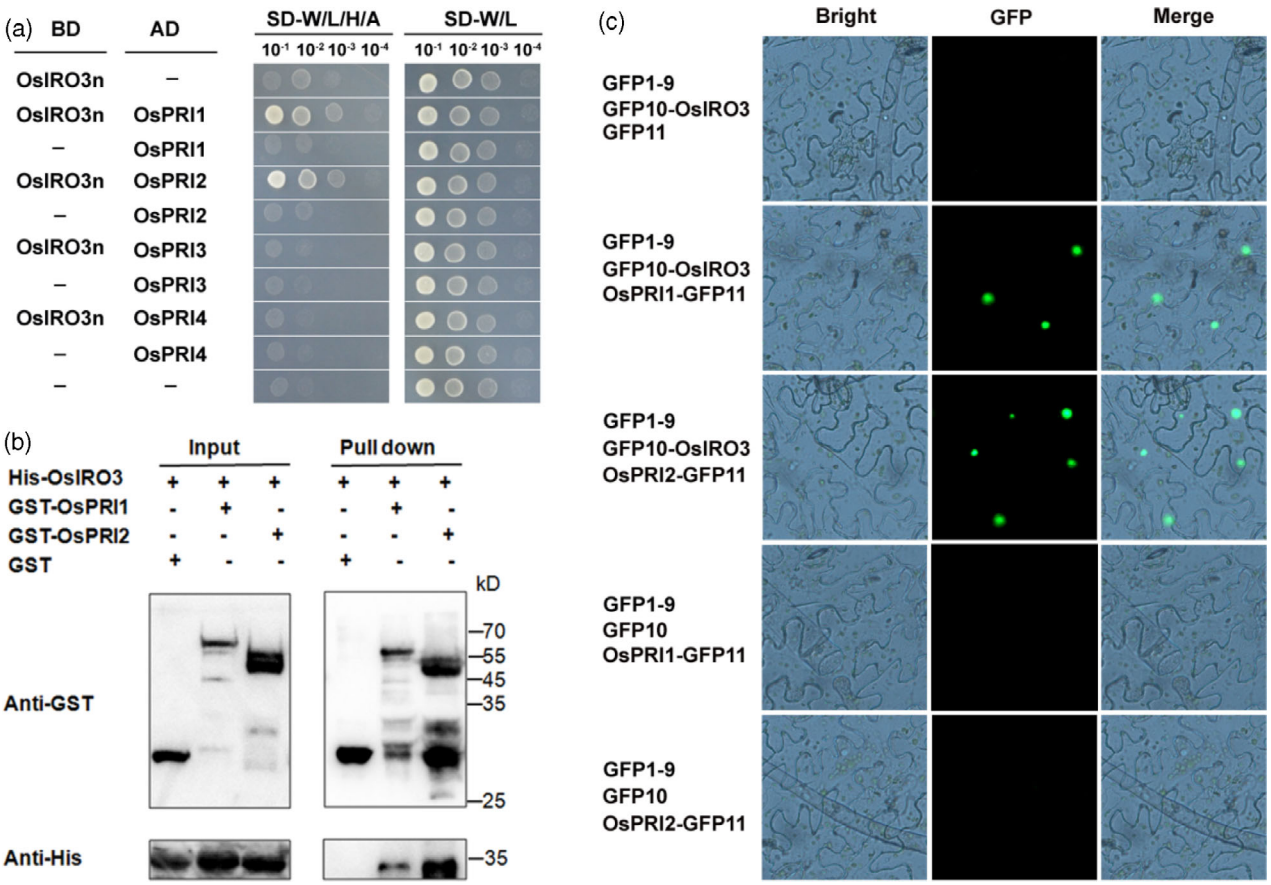

Figure 4. OsIRO3 physically interacts with OsPRI1 and OsPRI2.
(a) Yeast two-hybrid analysis of the interactions between OsIRO3 and OsPRI1/2. Yeast cotransformed with different binding domain (BD) and activating domain (AD) plasmid combinations was spotted on synthetic dropout medium lacking Leu/Trp (SD-W/L) or Trp/Leu/His/Ade (SD-W/L/H/A).
(b) Pull-down assays. OsPRI1/2 were respectively fused with the GST tag, and OsIRO3 was fused with the His tag. Recombinant proteins were expressed in *Escherichia coli*. Proteins were pulled down by glutathione Sepharose 4B and detected using the anti-His or anti-GST antibody.
(c) Protein interactions of OsIRO3 and OsPRI1/2 in plant cells. Tripartite split-sfGFP complementation assays were performed. OsPRI1 and OsPRI2 were respectively fused with GFP11, and OsIRO3 with GFP10. The constructs were introduced into Agrobacterium respectively, and the indicated combinations were co-expressed in *Nicotiana benthamiana* leaves.

interactions (Figure 6b). Given that the N-terminal of OsTPL/OsTPRs is responsible for the interaction with EAR motifs, three N-terminal truncated OsTPLn, OsTPR1n, and OsTPR2n were respectively fused with the BD. The full length of OsIRO2 and OsIRO3 were respectively fused with the activating domain. The results showed that OsIRO3, but not OsIRO2, could interact with OsTPL/OsTPRs, which is consistent with the fact that OsIRO3 is a negative regulator and OsIRO2 a positive regulator. To investigate further whether the EAR motif of OsIRO3 is responsible for the interactions with OsTPL/OsTPRs, we constructed a mutated version of OsIRO3 (OsIRO3m) with a mutated EAR motif (LxAxL). Interaction tests indicated that the mutation of EAR enabled OsIRO3m not to interact with OsTPL/OsTPRs, suggesting that the EAR motif is required for the interactions. Next, we performed pull-down assays in which OsTPLn was used as a representative (Figure 6c). The results suggest that OsTPLn could pull down OsIRO3. The tripartite split-GFP assays further confirmed that their interaction occurs in the nucleus (Figure 6d). Taken together, these results indicated that OsIRO3 interacts with OsTPL/OsTPRs co-repressors and its EAR motif is responsible for the interactions.

Repression function of OsIRO3 partially depends on its EAR motif

Having confirmed that OsIRO3 interacts with OsTPL/OsTPRs through its EAR motif, we asked if the EAR motif is crucial for the repression function of OsIRO3. To test this, we carried out the reporter-effector transient expression assays, in which Pro_{OsIRO2}:*nGFP* was used as the reporter. OsIRO3 strongly reduced the expression of *GFP* whereas OsIRO3m displayed a weak inhibitory effect on the expression of *GFP*. We further examined the influence of OsIRO3m on OsPRI1. When co-expressed with OsPRI1, both OsIRO3 and OsIRO3m repressed the expression of

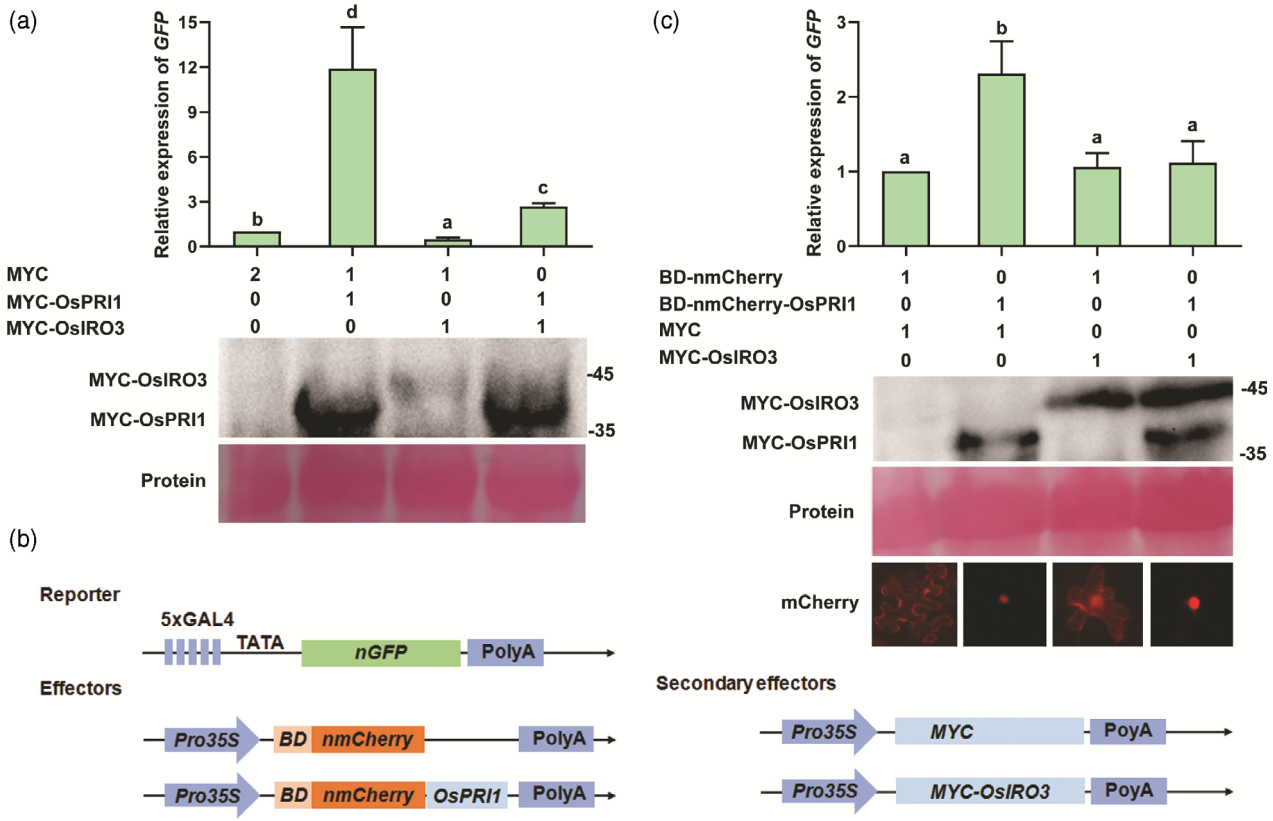

Figure 5. OsIRO3 antagonizes the transcriptional activation ability of OsPRI1.
(a) OsIRO3 represses the transcription activation of OsPRI1. The reporter and effectors are shown in Figure 3(b). Protein levels of effectors were detected by immunoblot. Ponceau staining shows equal loading. The *GFP/NPTII* ratio represents the *GFP* levels relative to the internal control *NPTII*.
(b) Schematic representation of the constructs used for transient expression assays. In the reporter, five repeats of GAL4 binding motif and the minimal CaMV 35S promoter was used as the promoter to drive the nGFP. In the effectors, BD-nmCherry and BD-nmCherry-OsPRI1 are under the control of 35S promoter. In the secondary effectors, MYC and MYC-OsIRO3 are under the control of 35S promoter.
(c) OsIRO3 inhibits the transcriptional activation ability of OsPRI1 by direct protein–protein interaction. Protein levels of effectors were detected by immunoblot. Ponceau staining shows equal loading. The abundance of *GFP* was normalized to that of *NPTII*. The value with the control (nmCherry) was set to 1. Different letters above each bar indicate statistically significant differences as determined by one-way ANOVA followed by Tukey's multiple comparison test ($P < 0.05$).

GFP compared with the control (MYC), but the inhibitory effect of OsIRO3m was not as strong as that of OsIRO3 (Figure 7a). These data suggest that the repression function of OsIRO3 is partially dependent on its EAR motif.

Given that the EAR motif affects the repression function of OsIRO3, we wanted to know whether the EAR motif also affects its biological functions. For this aim, we constructed transgenic plants overexpressing *OsIRO3* and *OsIRO3m*, respectively (Figure S2). Under Fe-sufficient conditions, both *OsIRO3-OX* and *OsIRO3m-OX* plants grew as well as the wild-type plants (Figure 7b). Under Fe-deficient conditions, two independent *OsIRO3* overexpression lines (*OE9* and *OE10*) showed hypersensitivity to Fe deficiency compared with the wild-type plants, including chlorotic leaves and reduced shoot height, which is consistent with the previous study (Zheng et al., 2010). Although the *OsIRO3m* overexpression lines (*mOE-1* and *mOE-14*) also displayed sensitivity to Fe deficiency, they were less sensitive to Fe deficiency compared with the *OsIRO3* overexpression plants. Taken together, our results suggest that the EAR motif is necessary for the biological functions of OsIRO3.

DISCUSSION

Plants have evolved intricate mechanisms to maintain Fe homeostasis. When facing Fe deficiency conditions, plants upregulate the expression of Fe deficiency inducible genes, thereby promoting Fe absorption to meet the plant's needs. However, excessive Fe uptake is likely to result in reactive oxygen species (ROS), which are toxic to plant cells. The balance between positive regulatory factors to activate the Fe uptake system and negative regulatory factors to suppress it maintains Fe homeostasis in plants. OsIRO2 is a crucial regulator of the Fe uptake system in rice. To maintain Fe homeostasis, rice plants activate *OsIRO2* under Fe-deficient conditions, and suppress it under Fe sufficient conditions. Previous studies have shown that OsPRI1/2/3 proteins positively regulate *OsIRO2* (Zhang et al., 2017, 2020). However, it was still unclear

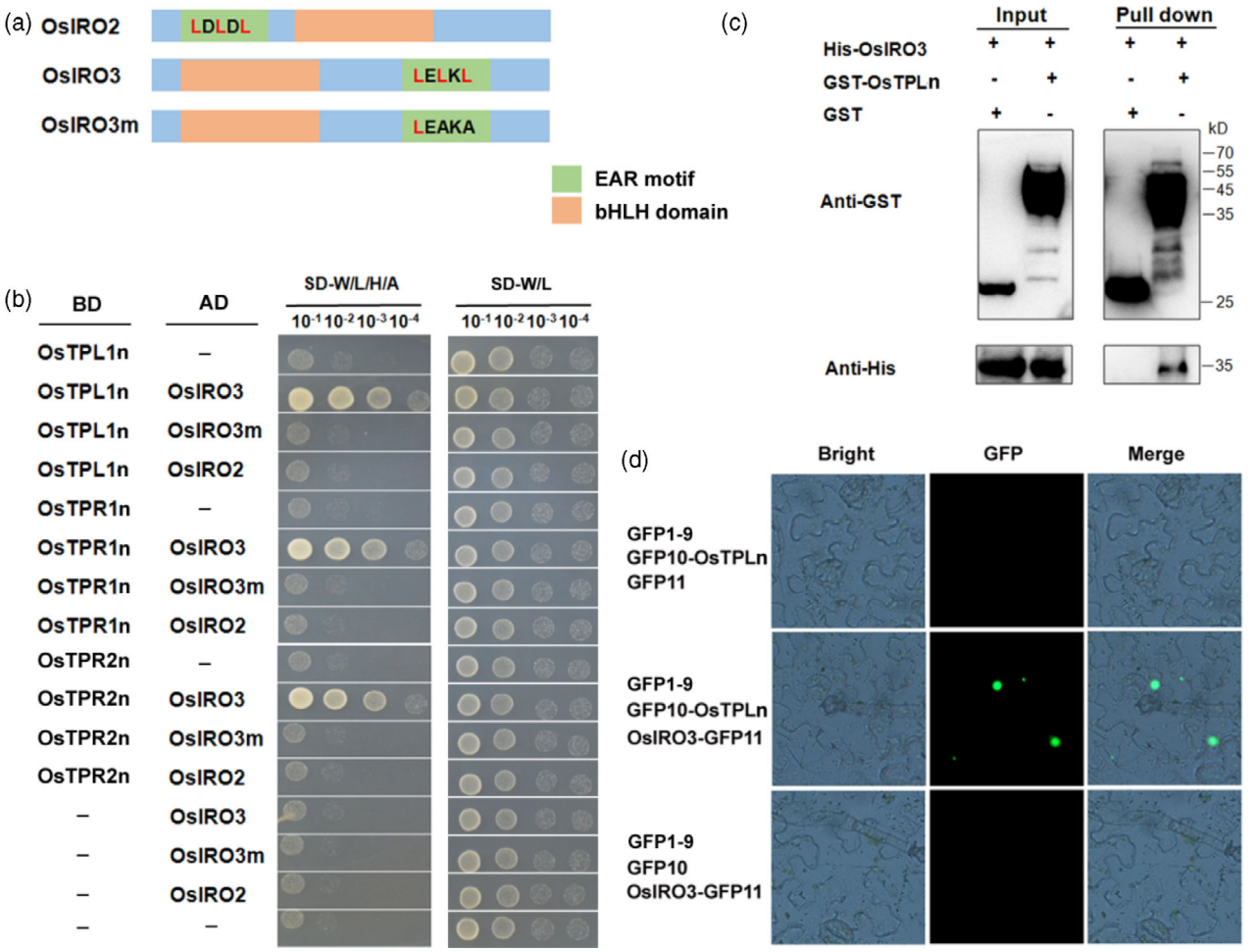

Figure 6. OsIRO3 interacts with the co-repressors OsTPL/OsTPRs.
(a) Schematic diagram of bHLH domain and EAR motif in the OsIRO2 and OsIRO3.
(b) EAR motif is required for the interactions between OsIRO3 and OsTPL/OsTPRs. Yeast cotransformed with different binding domain (BD) and activating domain (AD) plasmid combinations was spotted on synthetic dropout medium lacking Leu/Trp (SD-T/L) or Trp/Leu/His/Ade (SD-T/L/H/A).
(c) Pull-down assays. N-terminal of OsTPL was fused with the GST tag, and OsIRO3 was fused with the His tag. Recombinant proteins were expressed in *Escherichia coli*. Proteins were pulled down by glutathione Sepharose 4B and detected using the anti-His or anti-GST antibody.
(d) Interaction of OsIRO3 and OsTPLn in plant cells. Tripartite split-sfGFP complementation assays were performed. OsTPLn was fused with GFP10, and OsIRO3 with GFP11. The constructs were introduced into Agrobacterium respectively, and the indicated combinations were co-expressed in *Nicotiana benthamiana* leaves.

which transcription factors directly negatively regulate *OsIRO2*. Here, we provide evidence that OsIRO3 not only directly represses *OsIRO2* by associating with its promoter, but also indirectly by inhibiting the transcription activation of OsPRI1/2 to *OsIRO2*.

OsIRO3 was identified as a negative regulator of Fe homeostasis, as its overexpression leads to chlorotic leaves, decreased Fe concentration and reduced expression of many Fe deficiency inducible genes (Zheng et al., 2010). Recently, two different groups analyzed the *iro3* loss-of-function mutants. Wang, Itai, et al. (2020) showed that the expression of Fe deficiency inducible genes was increased in *iro3* under Fe-deficient conditions, and Wang, Ye, et al. (2020) did not observe the change of those genes except for *OsNAS3*. It is very likely that the different results are attributed to their different experimental conditions. Our results support that the loss-of-function of *OsIRO3* promotes the expression of Fe deficiency inducible genes. Similar to the previous findings, the loss-of-function of *OsIRO3* causes enhanced shoot Fe accumulation and necrotic spots in leaves under Fe-deficient conditions (Figure 1b,c). Those two groups have proved that the increased ROS contributes to the leaf necrosis of *iro3* mutants (Wang, Itai, et al., 2020; Wang, Ye, et al., 2020). It is noteworthy that OsbHLH061, a homolog of OsIRO3, also negatively regulates the expression of Fe deficiency inducible genes, but the *bhlh061* mutants do not produce necrotic spots in leaves (Wang et al., 2022), implying that

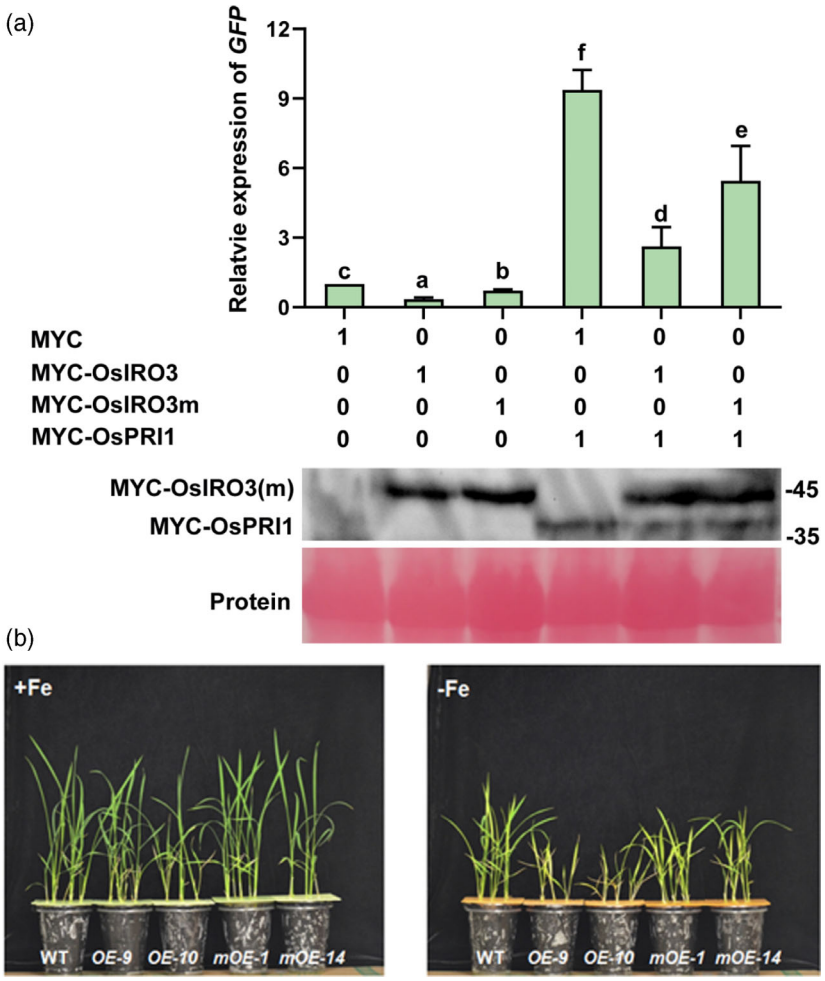

Figure 7. EAR motif partially contributes to the repression function of OsIRO3.
(a) EAR motif is partially required for the repression function of OsIRO3. Reporter and effectors are shown in Figure 3(b). Protein levels of effectors were detected by immunoblot. Ponceau staining shows equal loading. Abundance of *GFP* was normalized to that of *NPTII*. Value with the empty vector as an effector was set to 1. Different letters above each bar indicate statistically significant differences as determined by one-way ANOVA followed by Tukey's multiple comparison test ($P < 0.05$).
(b) Phenotypes of *OsIRO3*(*m*) overexpression plants. Seeds were germinated on wet paper for 7 days, and then seedlings were shifted in +Fe (0.1 mM Fe^{3+}) or −Fe (Fe free) solution for 2 weeks. WT, wild type.

OsIRO3 specifically represses ROS production in leaves under Fe-deficient conditions. Further investigation is needed to clarify how OsIRO3 regulates ROS production.

When plants are Fe deficient, they stimulate their Fe uptake systems to acquire more Fe. The fine-tuning of the Fe uptake system ensures the viability of cells, hence the health of plants. As a key regulator of the Fe uptake system, the transcription of *OsIRO2* must be tightly regulated. It has been revealed how the transcription of *OsIRO2* is activated directly under Fe-deficient conditions (Zhang et al., 2017, 2020). It was unclear how the transcription of *OsIRO2* is repressed directly. Our data suggest that OsIRO3 directly recognizes the *OsIRO2* promoter (Figure 3a), and represses the transcription of *OsIRO2* (Figure 3c). In addition to the direct repression, OsIRO3 also indirectly represses the transcription of *OsIRO2*, as OsIRO3 interacts with OsPRI1/2 to attenuate their transactivation activity towards *OsIRO2* (Figure 5a). Wang et al. (2022) also reported that OsbHLH061 negatively regulates *OsIRO2* by inhibiting the transcription activation of OsPRI1. Similar to *iro3*, the *bhlh061* mutants also accumulate more Fe in the shoot under Fe-deficient conditions. *OsIRO2* and its downstream genes are induced in the roots of *iro3* and *bhlh061* mutants regardless of Fe status (Figure 2; Wang et al., 2022). Thus, the repression function of both OsIRO3 and OsbHLH061 is required for maintaining Fe homeostasis.

OsIRO3 is a negative regulator of Fe homeostasis; however, it was unclear how OsIRO3 exerts its repressive function. There are two types of transcriptional repressors, active and passive repressors. Active transcriptional repressors function by recruiting the transcriptional corepressors, such as OsTPL/OsTPRs, while passive repressors compete with positive transcription factors for binding to target gene promoters. Here, we reveal that OsIRO3 can act as an active repressor by recruiting the transcriptional corepressors, OsTPL/OsTPRs (Figure 6). Our EMSAs confirmed that OsIRO3 could bind to the *OsIRO2* promoter, which is also targeted by OsPRI1/2/3 (Zhang et al., 2017, 2020). It raises the possibility that OsIRO3 competes with OsPRI1/2/3 for binding to the *OsIRO2* promoter so that less OsPRI proteins are involved in the transcription initiation

of *OsIRO2*. Therefore, OsIRO3 might also act as a passive repressor.

OsIRO2 is an ortholog of Arabidopsis bHLH Ib subgroup members (AtbHLH38, AtbHLH39, AtbHLH100, and AtbHLH101). Arabidopsis bHLH Ib subgroup members interact with AtFIT to modulate the expression of Strategy I genes (Wang et al., 2013; Yuan et al., 2008) while OsIRO2 interacts with OsFIT to control the expression of Strategy II genes (Liang et al., 2020; Wang, Li, et al., 2020). Arabidopsis bHLH IVc proteins directly regulate bHLH Ib genes (Li et al., 2016; Liang et al., 2017; Zhang et al., 2015) while rice bHLH IVc proteins directly target *OsIRO2* (Zhang et al., 2017, 2020). We reveal that OsIRO3 functions as a brake to restrict the expression of *OsIRO2* under Fe-deficient conditions. OsbHLH061 also recruits OsTPL/OsTPRs to inhibit the transcription activation of OsPRI1 towards *OsIRO2*. Unlike *OsbHLH061*, which is repressed by Fe deficiency, *OsIRO3* is induced. We propose that OsbHLH061 and OsIRO3 mainly function under Fe-sufficient and Fe-deficient conditions, respectively (Figure 8). A latest study revealed that AtbHLH11 recruits the co-repressors AtTPL/AtTPRs to regulate the Arabidopsis Fe homeostasis negatively (Li et al., 2022). Although rice and Arabidopsis utilize different strategies to take up Fe from soil, they have evolved this conserved regulatory mechanism to control the Fe uptake systems.

OsIRO3 is a close homolog of Arabidopsis AtPYE (POPEYE/AtbHLH47) (Zheng et al., 2010). AtPYE directly targets *AtZIF1*, *AtFRO3*, and *AtNAS4*, which are involved in Fe homeostasis (Long et al., 2010). Similarly, OsIRO3 directly regulates *OsNAS3* in rice (Wang, Ye, et al., 2020). Arabidopsis bHLH IVc subgroup members (AtbHLH34, AtbHLH104, AtbHLH105, and AtbHLH115) correspond to rice bHLH IVc subgroup members (OsPRI1, OsPRI2, OsPRI3, and OsPRI4) (Zhang et al., 2020). Similar to AtPYE, which physically interacts with three bHLH IVc members, AtbHLH104/105/115 (Long et al., 2010; Selote et al., 2015), OsIRO3 interacts with two bHLH IVc members, OsPRI1/2 (Figure 4). Although AtPYE and OsIRO3 share these similarities, they regulate Fe homeostasis in different manners. Unlike the *iro3* mutant plants, which accumulate more Fe only in the shoot under Fe-deficient conditions, *pye* mutant plants accumulate more Fe both in the root and shoot irrespective of Fe status (Long et al., 2010). Loss-of-function of

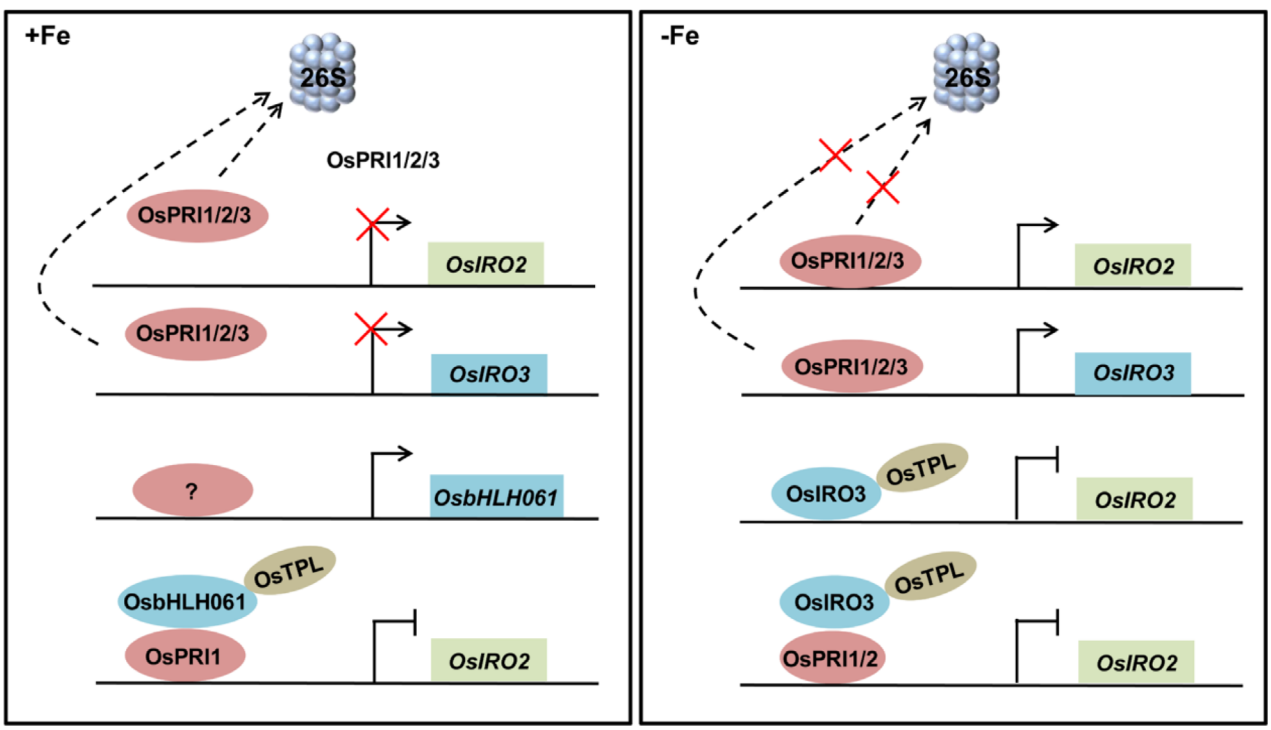

Figure 8. Transcription regulation of *OsIRO2* in Fe homeostasis.
OsPRI1/2/3 proteins undergo 26S proteasome-mediated degradation. OsPRI1/2/3 directly activates the promoters of *OsIRO2* and *OsIRO3*. OsIRO3 directly represses the promoter of *OsIRO2*. OsbHLH061 physically interacts with OsPRI1, and OsIRO3 with OsPRI1/2. Under Fe sufficient conditions, OsPRI1/2/3 may be degraded. On the other hand, *OsbHLH061* transcription is activated by unknown transcription factors and OsbHLH061 protein recruits the OsTPL co-repressor (OsTPL/OsTPRs) to inhibit the transcription activation of OsPRI1 to *OsIRO2*. Thus, both *OsIRO2* and *OsIRO3* are less expressed under Fe sufficient conditions. Under Fe-deficient conditions, the degradation of OsPRI1/2/3 may be repressed, which results in the upregulation of *OsIRO2* and *OsIRO3*. On the other hand, OsIRO3 negatively regulates the expression of *OsIRO2* by two ways, i.e., (i) OsIRO3 directly binds to the OsIRO2 promoter and recruits OsTPL to the transcription of OsIRO2, and (ii) OsIRO3 recruits OsTPL to inhibit the transcription activation of OsPRI2/3 towards *OsIRO2*.

AtPYE does not affect the expression of Fe uptake genes, such as *AtIRT1* and *AtFRO2* (Long et al., 2010), whereas the loss-of-function of *OsIRO3* facilitates the expression of Fe uptake genes. Thus, there is a functional divergence between OsIRO3 and AtPYE, and Arabidopsis and rice have developed different regulatory mechanisms to repress bHLH Ib genes.

This study expands our knowledge of the Fe homeostasis transcription network mediated by the OsIRO3-OsIRO2 module. Based on previous knowledge and our new findings, we propose a putative mechanism in which *OsIRO2* is regulated antagonistically (Figure 8). Under Fe-sufficient conditions, *OsbHLH061* transcription is activated and its protein recruits OsTPL/OsTPRs to inhibit the transcription activation of OsPRI1 towards *OsIRO2*. Under Fe-deficient conditions OsPRI1/2/3 protein may increase and activate the transcription of *OsIRO2* and *OsIRO3*. Meanwhile OsIRO3 recruits the co-repressors OsTPL/OsTPRs to represses *OsIRO2* in two different ways, i.e., (i) directly binding to the *OsIRO2* promoter to repress its transcription, and (ii) inhibiting the transcription activation of OsPRI1/2 towards *OsIRO2*. This work enhances our understanding of the Fe deficiency response signaling pathway in rice.

EXPERIMENTAL PROCEDURES

Plant materials and growth conditions

Rice cultivar "Nipponbare" was used in this study. Plants were grown in a greenhouse with a photoperiod of 14 h light 28°C and 10 h dark at 22°C. For hydroponic culture assays, Fe-sufficient solution was prepared in half-strength Murashige and Skoog with 0.1 mM Fe(III)-EDTA and Fe-deficient solution in the same media without Fe.

Generation of transgenic plants

The editing vectors were constructed as described previously (Liang et al., 2016). Two different target sites for *OsIRO3* were designed. The *OsU6a* promoter driving the sgRNA containing a specific target site was cloned into the pMH-SA vector by the restriction enzyme sites *Spe*I and *Asc*I. Two independent constructs were used for rice transformation. Homozygous mutant lines were identified by polymerase chain reaction (PCR) sequencing.

For the construction of overexpression vectors, HA-OsIRO3 and HA-OsIRO3m were amplified from GAD-OsIRO3 and GAD-OsIRO3m, respectively, and cloned between the maize ubiquitin promoter and the nitric oxide synthase terminator in the pUN1301 binary vector.

EMSA

OsIRO3 was cloned into the pET-28a(+) vector and the resulting plasmids was introduced into *E. coli* BL21(DE3) for protein expression. Cultures were incubated with 0.5 M isopropyl β-D-1-thiogalactopyranoside at 22°C for 16 h, and proteins were extracted and purified by using the His-tag Protein Purification Kit (Beyotime, Shanghai, China) following the manufacturer's protocol. EMSA was performed using the Chemiluminescent EMSA Kit (Beyotime) following the manufacturer's protocol. Briefly, two complementary single-strand DNA primers were synthesized with a biotin label at the 5′ end. Two complementary primers were mixed and annealed to form the biotin probe. The two biotin-unlabeled single-strand DNA primers were used as competitors, and the His protein alone was used as the negative control.

Reverse transcription and quantitative PCR

Total RNA extracted from rice roots using TRIzol reagent (Invitrogen, Carlsbad, CA, USA). cDNA was synthesized by the use of PrimeScript™ RT reagent Kit with gDNA Eraser (Perfect Real Time) according to the reverse transcription protocol (Takara, Dalian, China). The resulting cDNA was subjected to relative quantitative PCR using a SYBR Premix Ex Taq™ kit (TaKaRa) on a Roche LightCycler 480 real-time PCR machine, according to the manufacturer's instructions. All PCR amplifications were performed in three biological replicates with *OsACTIN1* and *OsOBP* as the internal controls. Primers used in this paper are listed in Supplementary Table S1.

Fe measurement

To determine Fe concentration, 14-day-old seedlings grown in half-strength Murashige and Skoog assay liquid with 0.1 mM Fe (III)-EDTA were transferred to Fe-sufficient (0.1 mM Fe(III)-EDTA) or Fe-deficient (Fe-free) liquid media for 7 days. The shoots and roots were harvested separately and dried at 65°C for 3 days. For each sample, about 500 mg dry weight of roots or shoots was digested with 5 ml of 11 M HNO_3 and 2 ml of 12 M H_2O_2 for 30 min at 220°C. Fe concentration was measured using inductively coupled plasma mass spectrometry.

Yeast two-hybrid assays

For yeast two-hybrid assays, the N-terminal truncated version of OsIRO3n, OsTPLn, OsTPR1n, and OsTPR2n were respectively cloned into pGBKT7. The sequence encoding full-length OsPRI1, OsPRI2, OsIRO2, OsIRO3, and OsIRO3m were respectively cloned into pGADT7. Vectors were transformed into yeast strain Y2HGold (Clontech, Mountain View, CA, USA). Growth was determined as described in the Yeast Two-Hybrid System User Manual (Clontech).

Protein interaction in plant cells

The GFP1-9, GFP10, and GFP11 sequences of superfolder GFP were cloned into separate pER8 vectors under the estradiol induction promoter, generating pTG-GFP1-9, pTG-GFP10, and pTG-GFP11, respectively. OsIRO3 and OsTPLn were cloned into pTG-GFP10 with an N-terminal GFP10 tag, and OsPRI1/2 and OsIRO3 were cloned into pTG-GFP11 with a C-terminal GFP11 tag. All vectors were introduced into *Agrobacterium tumefaciens* (strain EHA105) and various combinations of *Agrobacterium* cells were infiltrated into leaves of *N. benthamiana* in infiltration buffer (0.2 mM acetosyringone, 10 mM $MgCl_2$, and 10 mM MES [pH 5.6]). Gene expression was induced 1 day after agroinfiltration by injecting 20 mM β-estradiol into the abaxial side of the leaves. Epidermal cells were observed and recorded under a Carl Zeiss Microscope.

Pull-down assays

OsPRI1/2 and OsTPLn were cloned into pGEX-4T-1 respectively, and OsIRO3 was cloned into pET-28a(+). All plasmids were introduced into *E. coli* BL21 cells (TransGen Biotech). GST, GST-OsPRI1/2, GST-OsTPLn, and His-OsIRO3 proteins were induced by

0.1 mM isopropyl β-D-1-thiogalactopyranoside at 16°C for 20 h. Soluble GST, GST-OsPRI1/2, and GST-OsTPL-N were extracted and immobilized to glutathione affinity resin (Beyotime Biotechnology). For pull-down assays, His-OsIRO3 fusion proteins purified from *E. coli* cell lysate were incubated with the immobilized GST, GST-OsPRI1/2, and GST-OsTPLn in GST pull-down protein binding buffer (50 mM Tris–HCl, pH 8.0, 200 mM NaCl, 1 mM EDTA, 1% NP-40, 1 mM DTT, 10 mM $MgCl_2$, 1× protease inhibitor cocktail from Roche, Basel, Switzerland) for 2 h at 4°C. Proteins were eluted in the elution buffer, and the interaction was determined by Western blot using anti-His antibody and anti-GST antibody (TransGen Biotech, Beijing, China).

Transient expression assays

The nGFP driven by a synthetic promoter, which consists of five repeats of GAL4 binding motif and the minimal CaMV 35S promoter was described previously (Li et al., 2022). The GAL4 DNA binding domain was fused with mCherry containing a nuclear localization signal to generate 35S:BD-nmCherry. OsPRI1 was fused with BD-nmCherry as the effector. The promoter of OsIRO2 was used to drive nGFP as a reporter.

The promoter of *OsIRO2* was used to drive nGFP as a reporter. MYC-OsIRO3(m) and MYC-OsPRI1 were respectively cloned downstream of the 35S promoter to generate 35S:MYC-OsIRO3(m) and 35S:MYC-OsPRI1 as effectors.

Agrobacterium tumefaciens strain EHA105 was used for plasmid transformation. Agrobacterial cells were infiltrated into leaves of *N. benthamiana* by the infiltration buffer (0.2 mM acetosyringone, 10 mM $MgCl_2$, and 10 mM MES, pH 5.6). For transcription activation assay, the final optical density at 600 nm value was 1.5. Agrobacteria were mixed at the ratio as indicated and a final concentration of 0.2 mM acetosyringone was added. After infiltration, plants were placed in the dark at 24°C for 48 h before fluorescence observation and RNA extraction. The transcript abundance of *GFP* was normalized to *NPTII*.

Western blot

For total protein extraction, samples were ground to a fine powder in liquid nitrogen and then resuspended and extracted in protein extraction buffer (50 mM Tris, 150 mM NaCl, 1% NP-40, 0.5% sodium deoxycholate, 0.1% sodium dodecyl sulfate, 1 mM PMSF, 1× protease inhibitor cocktail [pH 8.0]). Sample was loaded on to 12% sodium dodecyl sulfate–polyacrylamide gel electrophoresis gels and transferred on to nitrocellulose membranes. The membrane was blocked with TBST (10 mM Tris-Cl, 150 mM NaCl, and 0.05% Tween 20, pH 8.0) containing 5% nonfat milk (TBSTM) at room temperature for 60 min and incubated with primary antibody in TBSTM (overnight at 4°C). Membranes were washed with TBST (three times for 5 min each) and then incubated with the appropriate horseradish peroxidase-conjugated secondary antibodies in TBSTM at room temperature for 1.5 h. After washing three times, bound antibodies were visualized with ECL substrate.

ACKNOWLEDGMENTS

We thank the Institutional Center for Shared Technologies and Facilities of Xishuangbanna Tropical Botanical Garden, CAS for assistance in the determination of metal contents. We also thank the Crops Conservation and Breeding Base of XTBG for rice planting. This work was supported by the National Natural Science Foundation of China (32001533).

AUTHOR CONTRIBUTIONS

GL conceived the project. CL and YL constructed plasmids. CL characterized plants, determined gene and protein expression, and conducted cellular assays. CL, YL, and PX grew rice and analyzed data. CL and GL wrote the manuscript. All authors discussed and approved the manuscript.

CONFLICT OF INTERESTS

The authors declare that they have no competing interests.

DATA AVAILABILITY STATEMENT

All relevant data can be found within the manuscript and its supporting materials.

SUPPORTING INFORMATION

Additional Supporting Information may be found in the online version of this article.

Figure S1. OsIRO3 does not bind to the promoter of OsFIT.

Figure S2. Expression of OsIRO3(m) in the overexpression plants.

Table S1. Primers used in this paper.

REFERENCES

Balk, J. & Schaedler, T.A. (2014) Fe cofactor assembly in plants. *Annual Review of Plant Biology*, **65**, 125–153.

Bashir, K., Nozoye, T., Nagasaka, S., Rasheed, S., Miyauchi, N., Seki, M. *et al.* (2017) Paralogs and mutants show that one DMA synthase functions in iron homeostasis in rice. *Journal of Experimental Botany*, **68**, 1785–1795.

Briat, J.F., Dubos, C. & Gaymar, F. (2015) Fe nutrition, biomass production, and plant product quality. *Trends in Plant Science*, **20**, 1360–1385.

Causier, B., Ashworth, M., Guo, W. & Davies, B. (2012) The TOPLESS interactome: a framework for gene repression in *Arabidopsis*. *Plant Physiology*, **158**, 423–438.

Cheng, L., Wang, F., Shou, H., Huang, F., Zheng, L., He, F. *et al.* (2007) Mutation in nicotianamine aminotransferase stimulated the Fe(II) acquisition system and led to iron accumulation in rice. *Plant Physiology*, **145**, 1647–1657.

Fisher, F. & Goding, C.R. (1992) Single amino acid substitutions alter helix-loop-helix protein specificity for bases flanking the core CANNTG motif. *The EMBO Journal*, **11**, 4103–4109.

Guerinot, M.L. & Yi, Y. (1994) Iron: nutritious, noxious, and not readily available. *Plant Physiology*, **104**, 815–820.

Hänsch, R. & Mendel, R.R. (2009) Physiological functions of mineral micronutrients (cu, Zn, Mn, Fe, Ni, Mo, B, cl). *Current Opinion in Plant Biology*, **12**, 259–266.

Inoue, H., Higuchi, K., Takahashi, M., Nakanishi, H., Mori, S. & Nishizawa, N.K. (2003) Three rice nicotianamine synthase genes, OsNAS1, OsNAS2, and OsNAS3 are expressed in cells involved in long-distance transport of iron and differentially regulated by iron. *The Plant Journal*, **36**, 366–381.

Inoue, H., Kobayashi, T., Nozoye, T., Takahashi, M., Kakei, Y., Suzuki, K. *et al.* (2009) Rice OsYSL15 is an Fe-regulated Fe (III)-deoxymugineic acid transporter expressed in the roots and is essential for Fe uptake in early growth of the seedlings. *The Journal of Biological Chemistry*, **284**, 3470–3479.

Ishimaru, Y., Suzuki, M., Tsukamoto, T., Suzuki, K., Nakazono, M., Kobayashi, T. *et al.* (2006) Rice plants take up Fe as an Fe^{3+}-phytosiderophore and as Fe^{2+}. *The Plant Journal*, **45**, 335–346.

Kagale, S., Links, M.G. & Rozwadowski, K. (2010) Genome-wide analysis of ethylene-responsive element binding factor-associated amphiphilic repression motif-containing transcriptional regulators in Arabidopsis. *Plant Physiology*, **152**, 1109–1134.

Kobayashi, T., Nagasaka, S., Senoura, T., Itai, R.N., Nakanishi, H. & Nishizawa, N.K. (2013) Fe-binding haemerythrin RING ubiquitin ligases

regulate plant Fe responses and accumulation. *Nature Communications*, **4**, 2792.

Kobayashi, T., Ozu, A., Kobayashi, S., An, G., Jeon, J.S. & Nishizawa, N.K. (2019) OsbHLH058 and OsbHLH059 transcription factors positively regulate Fe deficiency responses in rice. *Plant Molecular Biology*, **101**, 471–486.

Lee, S., Chiecko, J.C., Kim, S.A., Walker, E.L., Lee, Y., Guerinot, M.L. *et al.* (2009) Disruption of OsYSL15 leads to Fe inefficiency in rice plants. *Plant Physiology*, **150**, 786–800.

Li, X., Zhang, H., Ai, Q., Liang, G. & Yu, D. (2016) Two bHLH transcription factors, bHLH34 and bHLH104, regulate Fe homeostasis in *Arabidopsis thaliana*. *Plant Physiology*, **170**, 2478–2493.

Li, Y., Lei, R., Pu, M., Cai, Y., Lu, C., Li, Z. *et al.* (2022) bHLH11 inhibits bHLH IVc proteins by recruiting the TOPLESS/TOPLESS-RELATED corepressors. *Plant Physiology*, **188**, 1335–1349.

Liang, G., Zhang, H., Li, X., Ai, Q. & Yu, D. (2017) bHLH transcription factor bHLH115 regulates Fe homeostasis in *Arabidopsis thaliana*. *Journal of Experimental Botany*, **68**, 1743–1755.

Liang, G., Zhang, H., Li, Y., Pu, M., Yang, Y., Li, C. *et al.* (2020) *Oryza sativa* FER-LIKE FE DEFICIENCY-INDUCED TRANSCRIPTION FACTOR (OsFIT/OsbHLH156) interacts with OsIRO2 to regulate Fe homeostasis. *Journal of Integrative Plant Biology*, **62**, 668–689.

Liang, G., Zhang, H., Lou, D. & Yu, D. (2016) Selection of highly efficient sgRNAs for CRISPR/Cas9-based plant genome editing. *Scientific Reports*, **6**, 21451.

Long, T.A., Tsukagoshi, H., Busch, W., Lahner, B., Salt, D.E. & Benfey, P.N. (2010) The bHLH transcription factor POPEYE regulates response to Fe deficiency in *Arabidopsis* roots. *The Plant Cell*, **22**, 2219–2236.

Mori, S. (1999) Fe acquisition by plants. *Current Opinion in Plant Biology*, **2**, 250–253.

Nozoye, T., Nagasaka, S., Kobayashi, T., Takahashi, M., Sato, Y., Sato, Y. *et al.* (2011) Phytosiderophore efflux transporters are crucial for Fe acquisition in graminaceous plants. *The Journal of Biological Chemistry*, **286**, 5446–5454.

Ogo, Y., Itai, R.N., Nakanishi, H., Kobayashi, T., Takahashi, M., Mori, S. *et al.* (2007) The rice bHLH protein OsIRO2 is an essential regulator of the genes involved in Fe uptake under Fe-deficient conditions. *The Plant Journal*, **51**, 366–737.

Römheld, V. & Marschner, H. (1986) Evidence for a specific uptake system for Fe phytosiderophores in roots of grasses. *Plant Physiology*, **80**, 175–180.

Selote, D., Samira, R., Matthiadis, A., Gillikin, J.W. & Long, T.A. (2015) Fe binding E3 ligase mediates Fe response in plants by targeting basic helix-loop-helix transcription factors. *Plant Physiology*, **167**, 273–286.

Shojima, S., Nishizawa, N.K., Fushiya, S., Nozoe, S., Irifune, T. & Mori, S. (1990) biosynthesis of phytosiderophores: in vitro biosynthesis of 2′-deoxymugineic acid from l-methionine and nicotianamine. *Plant Physiology*, **93**, 1497–1503.

Toledo-Ortiz, G., Huq, E. & Quail, P.H. (2003) The *Arabidopsis* basic/helix-loop-helix transcription factor family. *The Plant Cell*, **15**, 1749–1770.

Valko, M., Morris, H. & Cronin, M.T. (2005) Metals, toxicity and oxidative stress. *Current Medicinal Chemistry*, **12**, 1161–1208.

Wang, F., Itai, R.N., Nozoye, T., Kobayashi, T., Nishizawa, N.K. & Nakanishi, H. (2020) The bHLH protein OsIRO3 is critical for plant survival and iron (Fe) homeostasis in rice (*Oryza sativa* L.) under Fe-deficient conditions. *Soil Science and Plant Nutrition*, **66**, 579–592.

Wang, N., Cui, Y., Liu, Y., Fan, H., Du, J., Huang, Z. *et al.* (2013) Requirement and functional redundancy of Ib subgroup bHLH proteins for Fe deficiency responses and uptake in *Arabidopsis thaliana*. *Molecular Plant*, **6**, 503–513.

Wang, S., Li, L., Ying, Y., Wang, J., Shao, J.F., Yamaji, N. *et al.* (2020) A transcription factor OsbHLH156 regulates strategy II Fe acquisition through localising IRO2 to the nucleus in rice. *The New Phytologist*, **225**, 1247–1260.

Wang, W., Ye, J., Ma, Y., Wang, T., Shou, H. & Zheng, L. (2020) OsIRO3 plays an essential role in iron deficiency responses and regulates iron homeostasis in Rice. *Plants (Basel)*, **9**, 1095.

Wang, W., Ye, J., Xu, H., Liu, X., Fu, Y., Zhang, H. *et al.* (2022) OsbHLH061 links TOPLESS/TOPLESS-RELATED repressor proteins with POSITIVE REGULATOR OF IRON HOMEOSTASIS 1 to maintain iron homeostasis in rice. *The New Phytologist*, **234**, 1753–1769. https://doi.org/10.1111/nph.18096

Yuan, Y., Wu, H., Wang, N., Li, J., Zhao, W., Du, J. *et al.* (2008) FIT interacts with AtbHLH38 and AtbHLH39 in regulating Fe uptake gene expression for Fe homeostasis in *Arabidopsis*. *Cell Research*, **18**, 385–397.

Zhang, H., Li, Y., Pu, M., Xu, P., Liang, G. & Yu, D. (2020) *Oryza sativa* POSITIVE REGULATOR OF FE DEFICIENCY RESPONSE 2 (OsPRI2) and OsPRI3 are involved in the maintenance of Fe homeostasis. *Plant, Cell & Environment*, **43**, 261–274.

Zhang, H., Li, Y., Yao, X., Liang, G. & Yu, D. (2017) POSITIVE REGULATOR OF FE HOMEOSTASIS1, OsPRI1, facilitates Fe HOMEOSTASIS. *Plant Physiology*, **175**, 543–554.

Zhang, J., Liu, B., Li, M., Feng, D., Jin, H., Wang, P. *et al.* (2015) The bHLH transcription factor bHLH104 interacts with IAA-LEUCINE RESISTANT3 and modulates Fe homeostasis in *Arabidopsis*. *The Plant Cell*, **27**, 787–805.

Zheng, L., Ying, Y., Wang, L., Wang, F., Whelan, J. & Shou, H. (2010) Identification of a novel Fe regulated basic helix-loop-helix protein involved in Fe homeostasis in *Oryza sativa*. *BMC Plant Biology*, **10**, 166.